1 **Seismic velocity deviation log: an effective method for evaluating spatial distribution of**

2 **reservoir pore types**

3   Mohamad Shirmohamadi[1]; Ali Kadkhodaie[2,3*]; Hossain Rahimpour-Bonab[1] and Mohammad Ali Faraji[1]

4 1. Department of Geology, College of Science, University of Tehran, Tehran, Iran

5 2. Department of Earth Science, Faculty of Natural Science, University of Tabriz, Iran

6 3. Department of Petroleum Engineering, Curtin University, Perth, Western Australia

7

8 **Abstract**:

9 Velocity deviation log (VDL) is a synthetic log used to determine pore types in reservoir rocks

10 based on a combination of the sonic log with neutron-density logs. The current study proposes a

11 two steps approach to create a map of porosity and pore type by integrating the results of

12 petrographic studies, well logs and seismic data. In the first step, velocity deviation log was created

13 from the combination of the sonic log with the neutron-density log. The results allowed identifying

14 negative, zero and positive deviations based on the created synthetic velocity log. Negative

15 velocity deviations (below -500 m/s) indicate connected or interconnected pores and fractures,

16 while positive deviations (above +500 m/s) are related to isolated pores. Zero deviations in the

17 range of [-500m/s, +500m/s] are in good agreement with intercrystalline and microporosities. The

18 results of petrographic studies were used to validate the main pore type derived from velocity

19 deviation log. In the next step, velocity deviation log was estimated from seismic data by using a

20 probabilistic neural network model. For this purpose, the inverted acoustic impedance along with

21 the amplitude based seismic attributes were formulated to VDL.

* Corresponding author. Tel.: +618 9266 9366
E-mail addresses: mshirmohamadi70@ut.ac.ir (M. Shirmohamadi), Kadkhodaie_ali@tabrizu.ac.ir &
ali.kadkhodaie@curitn.edu.au (A. Kadkhodaie), hrahimpor@gmail.com (H. Rahimpour-Bonab), m.faraji@ut.ac.ir (M.A. Faraji)

The methodology is illustrated by performing a case study from the Hendijan oilfield, northwestern Persian Gulf. The results of this study show that integration of petrographic, well logs and seismic attributes is an instrumental way for understanding the spatial distribution of main reservoir pore types.

1. Introduction

Carbonate reservoirs show higher complexity in comparison to their sandstone counterparts. This is due to their depositional heterogeneities inherited from lateral and vertical facies changes, which causing a complex pore type and size system (Wayne 2008). In addition, secondary diagenetic processes enhance these primary complexity and heterogeneity. Thus, one of the most important challenges in carbonate reservoir study is pore typing. Pore types determine the trend of permeability and using the velocity deviation log (VDL) can help petrophysicists to determine them from well logging data. Laboratory research shows that sonic wave velocity, in addition to volumes of porosity, depends on pore types. Velocity deviation log, as introduced by Anselmetti and Eberli (1999), is an important tool for pore typing of carbonate reservoirs.

Most productive Iranian petroleum reservoirs are carbonate reservoirs in which some diagenetic overprints such as compaction, anhydrite plugging, cementation and over dolomitization have reduced their quality during the geological time but fractures usually make them more prolific (Wayne 2008). These fractures generally playing the main role in reservoir permeability increase and production.

In recent years an increasing trend for incorporation of seismic data into petrophysical investigations and interpretations is observed (e.g. Ouenes, 2000; Hampson et al., 2001; Doyen

2007, Kadkhodaie-Ilkhchi et al., 2009, Dezfoolian et al., 2013, Yarmohammadi, et al., 2014; Nouri-Taleghani et al., 2015; Nourafkan and Kadkhodaie-Ilkhchi, 2015; Kosari et al., 2015, Golsanami et al., 2015). Through inversion of amplitude based seismic data to acoustic impedance, many geological and petrophysical interpretations can be made. Acoustic impedance is highly under the influence of density and sonic compressional velocity, that both related to rocks properties.

The Hendijan oilfield (Fig. 1) is located 55 kilometers west of Bahregan District, Persian Gulf. The Oligo-Miocene Asmari Formation is currently the main reservoir unit of the Hendijan oilfield. The mixed carbonate and siliciclastic interval of Asmari Formation is characterized by a transgressive-regressive cycle formed under shallow marine and marine marginal/lagoonal waters in an overall regressive environment. The carbonate interval represents a westward extension of the productive Asmari Formation and the Ghar sandstone corresponds to the Ahwaz Member deposited in an onshore environment.

The current study reaps the benefits of both core and log data to generate a most reliable pore type log for the Asmari Formation at three wells of the studied field. Afterward, seismic data are inverted to acoustic impedance and then correlation models are established between inversion results and the most relevant seismic attributes by using probabilistic neural networks to generate a section of porosity and pore types.

It is worth mentioning that the neural network model for rock properties estimation is not a novel topic and is mainly based on other researcher's work but it could be claimed that the current study is the first report of pore types determination from seismic data. The methodology is straightforward, robust and easy to implement.

2. Methodology

The current study proposes a two steps approach to create a map of porosity and pore types by integration of petrographic studies results, well logs and seismic data in the Asmari reservoir. In the first step, velocity deviation log is created from a combination of sonic log, neutron and density logs. Then, the results of velocity deviation log are validated by using petrographic studies results. In the next step, velocity deviation log is estimated from seismic data by using a probabilistic neural network model. For this purpose, intelligent formulations are made between inversion result (acoustic impedance) and the amplitude based seismic attributes.

Laboratory measurement on more than 300 samples reveals that sonic velocity in rocks in addition to porosity volume, highly depends on porosity types (Anselmetti and Eberli 1999). Actually, there is a negative correlation between porosity values and velocity. Frame-forming porosities (such as moldic or intra-fossil porosity), result in significantly higher velocity values at equal total porosities than porosities which are not embedded in a rigid rock frame, such as interparticle porosity or microporosity.

As defined by Anselmetti and Eberli (1999), velocity deviation log is defined as the difference between real and synthetic sonic velocity of rocks (Eq. 1).

$$VDL = (Vp - Vp_{syn}) \times 1000 \qquad \text{Eq. (1)}$$

Where VDL is velocity deviation (m/s), Vp is compressional velocity (Km/s) and Vp_{syn} is synthetic compressional velocity (Km/s).

Compressional and synthetic velocity are easily derived from sonic logs by using Eq. (2) & Eq. (3)

1     $Vp = \dfrac{304.8}{DT}$ Eq. (2)

2     $Vp_{syn} = \dfrac{304.8}{DT_{syn}}$ Eq. (3)

3   where DT is sonic log values in µs/ft and 304.8 is a conversion factor to calculate Vp in Km/s.

4   DT_{syn} in equation 3 refers to synthetic compressional velocity and is calculated mainly based on

5   Wyllie's equation (1956). The general form of Wyllie's equation is expressed as Eq. (4)

6     $DT = DT_m(1 - \varphi) + \varphi DT_f$ Eq. (4)

7   where φ is porosity, DT refers to sonic wave travel time measured by logging tool, DT_m and DT_f

8   are sonic wave travel time in rock matrix and fluid occupied flushed zone, respectively. They were

9   taken as 47, 55 and 189 µs/ft for sandstone, limestone and flushed zone fluid respectively

10   (Schlumberger, 2009).

11   To calculate porosity, Eq. (4) can be rearranged as below.

12    $\varphi = \dfrac{DT - DT_m}{DT_f - DT_m}$ Eq. (5)

13   As is seen, the aim of Eq. (5) is to determine unknown porosity from the known parameters of

14   sonic transit time measured by logging tool, fluid and matrix transit times.

15   Assuming that porosity is already determined from neutron or density log, Eq. (5) can be solved

16   to find X or synthetic sonic wave travel time as follows.

17    $\varphi_{ND} = \dfrac{X - DT_m}{DT_f - DT_m}$ Eq. (6)

To calculate X, Eq. (6) can be rearranged as below.

$$X = \varphi_{ND}(\ DT_f - DT_m) + DT_m \qquad\qquad \text{Eq. (7)}$$

The value derived from solving Eq. (1) is called velocity deviation and can either be a positive or a negative value. The magnitude of the velocity deviation positively or negatively is directly related to the pore types and their distribution in a reservoir rock.

Inversion of seismic data is a common method for estimating subsurface layers acoustic impedance from gathered seismic data. Using acoustic impedance could provide a meticulous geological interpretation in detail and prevent geoscientist from misleading about subsurface. Most petroleum companies use seismic inversion to reduce uncertainty in subsurface studies and to improve the estimation of reservoir rock properties such as porosity and lithology because of its performance and usefulness (Pramanik et al., 2002; Gavotti et al., 2012).

Probabilistic neural network (Wang et al., 2015) are now well-known methods to solve non-linear and complicated problems Many companies have now included neural network models in their commercial software packages. In the current study, they will be used as intelligent tools to estimate velocity deviation from seismic attributes. For this purpose, neural network tools of the MATLAB and Hampson Russell software available in the Curtin University of Western Australia (Perth) were used.

3. Application to the Hendijan oilfield

3.1. Calculating velocity deviation from porosity logs

In the first step, it was necessary to check well logs quality and make sure about their correctness. Well logs were checked for problems related to washouts, depth shifting, log tails, abnormal logging ranges and spikes. Afterwards, velocity deviation log was calculated throughout the

Asmari formation by using equations 1 through 7 from neutron, density and sonic log (Fig. 2). Velocity deviation log is shown in the left tracks of Fig. 2. Sonic and density logs are shown on the right tracks and the middle track represents NPHI log. Negative deviations indicate connected porosities and in some cases fractures, while positive deviations are indicative of isolated pore types such as moldic and vuggy porosity. Zero deviations show intercrystaline and micro-porosities.

In order to validate pore types derived from VDL, the result of petrographic studies were employed. Photomicrographs showing the main facies of Asmari formation along with their main pore types and velocity deviation are displayed in Fig. 3. As is seen, there is a good agreement between the pore types recommended by VDL log and those derived through thin-section studies. The main pore types identified within each microfacies are closely connected to their corresponding velocity deviation values. In the light of acceptable results of pore typing from a combination of log and core data, the velocity deviation logs were subjected to further study in a 2D profile based on seismic data.

3.2. Well to seismic tie

In this study, pots stack seismic lines of the Hendijan were employed to investigate the proposed methodology of pore typing based on seismic data. A snapshot of CDP gathers after processing is displayed in Fig. 4a. As is seen, the general quality of seismic data is good with frequencies ranging from 0 to 80 Hz (average 30 Hz). The main processing steps applied on raw seismic data include demultiplexing, despiking, trace normalization, normal move out, CMP Stack, migration and scaling. Firstly, well log data were correlated to seismic data. Synthetic seismograms were generated for the available wells including HD-01, HD-03 and HD-05. The acoustic velocities from the DT logs were multiplied by the RHOB values from density logs to derive the acoustic

1 impedance data. The acoustic impedance was mapped to reflection coefficient, which was then

2 transformed from depth to time by using a prober check shot velocity relation. Lastly, the reflection

3 coefficient in time was convolved with a suitable wavelet to generate a synthetic seismogram. The

4 transformation from depth to the time domain of the well logs was carried out by applying check

5 shot data available for the studied wells. It was necessary to create synthetics and extract the

6 wavelets iteratively for the placement of the log data in time. Such a process allowed for checking

7 the well logs and their associated formation tops with the composite seismic trace in time domain.

8 Composite trace, which is a single average trace around the borehole, is derived by averaging

9 neighboring traces. The averaging was defined by a neighborhood radius of 1, which means one

10 neighboring CDP away from the well was used in the averaging process. As an example, the

11 synthetic seismogram for well HD-03 is illustrated in Fig. 4b. As shown the correlation between

12 the synthetic seismogram in the blue and composite trace in red at the mentioned well location is

13 0.755.

14 **3.3. Inverting seismic data to acoustic impedance**

15 In this study, the main motivation to do seismic inversion is to provide an appropriate input for

16 pore type determination from a set of pre-defined seismic attributed.

17 The inversion process stated in this manuscript is the algorithm by which we analyze stacked

18 seismic traces and attempt to estimate and rebuild the velocity or impedance structure of the

19 earth. The fundamental model on which inversion is based is the 1-D convolutional model as

20 following.

$$T(i) = \sum_j r(j)\, W(i-j+1) + n(i)$$

Eq. (8)

21

22 Where $T(i)$: seismic trace, $r(j)$: zero-offset reflectivity of the earth expressed as a time series

W(i): seismic wavelet, assumed to be constant and n(i) is measurement noise

The inversion algorithm tries to remove the extracted wavelet, W(i), from seismic traces. This process is called deconvolution. By minimizing the observed difference between the synthetic seismogram and the composite trace the acoustic impedance is estimated. Accordingly, inversion is determining the reflectivity, r(j), given the seismic trace, T(i). Reflectivity results in acoustic impedance of a series of layers in the earth by

$$r(j) = \frac{I(j) - I(j-1)}{I(j) + I(j-1)}$$

Eq. (9)

where I(j) is acoustic impedance derived from multiplying density and velocity.

The acoustic impedance derived from seismic data has a strong relationship with porosity from corresponding pore types. For this purpose, first an initial geological model was created. Initial geological model is the basis for acoustic impedance inversion of seismic data. Actually, inversion algorithm modifies the initial geological model through different iterations until a good match is obtained between synthetic traces and seismic trace. It is a low frequency model created by interpolating well logs. Seismic horizons are used as a guide for interpolation of well logs as they show structural and stratigraphic constrains to the model.

After performing well to seismic tie and creating appropriate synthetic seismograms, an appropriate wavelet was extracted to be used in deconvolution process. All modern seismic inversion methods require seismic data and a wavelet estimated from the data. Typically, a reflection coefficient series from a well within the boundaries of the seismic survey is used to estimate the wavelet phase and frequency. Accurate wavelet estimation is critical to the success of any seismic inversion. The inferred shape of the seismic wavelet may strongly influence the seismic inversion results and, thus, subsequent assessments of the reservoir quality.

In this study, amplitude and phase spectra of wavelet were estimated statistically from a combination of seismic data and well controls for which sonic and density curves were available. The extracted wavelet was applied to estimate reflection coefficients. When the estimated constant phase of the wavelet is in good agreement with the final result, the wavelet estimation converges more quickly than the case of using a zero phase assumption. Errors in well to seismic tie can cause frequency or phase artifacts in the wavelet extraction process. The identified wavelet is used to create a synthetic reflection coefficient for every seismic trace. Finally, the estimated reflection coefficients are convolved with the extracted wavelet to generate synthetic seismic traces which are compared to the original seismic. The results of acoustic impedance inversion for one of 2D section from the Hendijan oilfield are displayed in Fig. 5. The inverted section is valid for the interval between Ghar top and Jahrum top for which wavelet has been extracted. Ghar member is the most prolific reservoir unit in the studied field. Well HD-03 cuts through the section and color legend represents the value of acoustic impedance variations.

3.4. Seismic attributes extraction

Acoustic impedance is an important attribute derived from seismic inversion. However, using the acoustic impedance alone does not seem to be a perfect way to predict reservoir pore type. The primary goal of seismic survey is to map the subsurface features and structures, properly. Assuming that the amplitudes of seismic traces are correctly obtained, a set of amplitude-based math calculation referred to as seismic attributes can be derived and used in interpretation. A set of twenty-four attributes such as instantaneous frequency, Hilbert transform, amplitude derivatives and dominant frequency were extracted from the available post-stack seismic data. Attributes are quantities which extracted from raw seismic data and can be very useful for estimating reservoir

1 rock properties. They were used to find the appropriate predictors besides inversion result in the

2 neural network structure to generate velocity deviation sections.

3.5.Extracting porosity and velocity deviation sections

4 The acoustic inversion seismic data together with the extracted seismic attributes were investigated

5 to find the appropriate set of inputs for estimation of porosity and velocity deviation. Correlation

6 between the acoustic impedance versus porosity and sonic travel time are shown in Fig. 6 & 7. As

7 is seen, porosity and DT log show an inverse relationship with acoustic impedance derived from

8 inversion result confirming the validity of inversion result. Accordingly, inversion results were

9 considered as the main input for velocity deviation mapping. There are many seismic attributes

10 that could be considered as inputs, but those with the least error in validation process were chosen

11 for training the neural network. The strategy for finding suitable attribute is to find the best single

12 attribute, then the best pair of attributes, then the best triplet of attributes, etc. At each stage, the

13 threshold for choosing the "best" set is based on the root mean square prediction error, i.e., the best

14 set is the one that estimates the target logs with the least RMS error (Hampson-Russell user's

15 guide, 2014).

16 In order to fix the resolution problem between well logs and seismic data a convolutional operator

17 (operator length= 5) was used. Each seismic attribute will repeat by the length of convolutional

18 operator through upward and downward shifting of all samples in that attribute. Having eight input

19 seismic attributes with operator length of five results in 40 seismic attributes. Each seismic

20 attribute will repeat five times through time samples shift of -2, −1, 0, +1 and +2. This approach,

21 which was proposed by Hampson et al. (2001), improved the efficiency of the well to seismic

22 mapping procedure. As is seen in Fig. 8, running the models for porosity estimation with operator

23 length = 5 proposes eight input predictor attributes including acoustic impedance, integrated

absolute amplitude, quadrature trace, instantaneous phase, amplitude weighted cosine phase, apparent polarity, filter 50/10-15/20 and amplitude envelope.

For the case of sonic transit time the nine optimal inputs (Fig. 9) including acoustic impedance, integrated absolute amplitude (amplitude), integrate, integrated absolute amplitude (AI), apparent polarity, integrate, amplitude weighted phase, second derivative instantaneous amplitude and second derivative were used in the neural network structure.

Although seismic attributes are mathematical calculation, following justifications can be made to link them to rock physics and pore types variations.

Acoustic impedance is the product of density and velocity showing the strongest correlation with both porosity and DT logs. Amplitude-based attributes such as integrated absolute amplitude, integrate, second derivative absolute amplitude, amplitude envelope, integrated absolute amplitude quadrature trace and frequency filters are related to changes in subsurface rocks lithology and porosity. Sharp changes in lithology and pore types can cause strong amplitude anomalies. Apparent polarity is sensitive to lateral changes of polarity along a seismic reflection. It is closely connected to reflection strength which is used to identify bright/dim/flat spots. Lateral porosity, lithology and fluid variations affect reflection polarity. Instantaneous phase and amplitude weighted phase are sensitive to pore types and acoustic impedance since they can cause local phasing.

A cross-validation method was used to prevent over-training problem and to measure the reliability of the models. That is, the training process was repeated as many times as there are wells, each time leaving out a different well dataset to measure the performance of the models. It is worth mentioning one of the main advantages of PNNs over other intelligent systems is their very limited parameter setting. For this reason, they less perform as black boxes. As is seen from the algorithm

of neural network (Appendix 1), the only parameter of the PNN which needs to be optimized is scale parameter (σ). Optimizing the scale parameter to 1.0 satisfactory results were obtained.

After selection of appropriate inputs and tuning and validating neural network models (Fig. 10 & 11) porosity and sonic transit time were estimated over the interval of interest. The rest of the process which includes seismic based velocity deviation calculations from estimated porosity and sonic travel time sections was done in MATLAB environment. For this purpose, seismic data with SEGY format were converted to ASCII format so that they can be read and stored in Matrix files of MATLAB. By using the graphical representation functions of MATLAB all results were visualized and interpreted. A flow chart showing the steps of creating a velocity deviation section is shown in Fig. 12.

4. Results and discussion

The results of seismic derived porosity and sonic transit time are shown in Figs. 13 and 14. Through performing a sequence of calculations by using equations 1 through 7 in MATLAB programming environment a section of velocity deviation was achieved (Fig. 15). Such a section is very useful in the interpretation of pore types distribution and changes in inter-well spaces. Seismic velocity deviation section can be used for pore typing. There is a good agreement between the pore types recommended by VDL log and those derived through thin-section studies. The main pore types identified within each microfacies are closely connected to their corresponding velocity deviation values. Accordingly, the reservoir rocks can be classified into three zones based on their velocity deviation values as follows.

Zones with positive deviations (VDL> +500 m/s), the estimated velocity is less than the sonic velocity which is in relation to the presence of isolated pores such and vuggy or moldic porosities.

Sonic logs are more sensitive to primary and connected porosities for which neutron and density logs measure higher porosities in comparison to sonic porosity causing a positive velocity deviation. They are characterized by red to green colors in the velocity deviation section shown in Fig. 15.

Zones with approximately zero deviation dedicated to zones with inter crystalline, inter granular and micro porosity, these pore types due to good sorting and connected pore throat usually indicate zones with good pore connectivity except micro porosity in which despite zero VDL amounts has low pore connections. They are characterized by small negative or positive deviation values (-500< VDL < +500 m/s) called zero deviations. They are characterized by light blue to blue colors in the velocity deviation section shown in Fig. 15.

Zone with negative deviations (VDL<-500 m/s) where that the estimated velocity based on neutron-density logs is more than the real velocity derived from the sonic log. Such a case happens in fractured rocks, gas bearing zones or rocks containing interconnected and connected pores for which a higher sonic travel time (lower velocity) is recorded. Accordingly, porosity derived from the sonic log is higher than neutron or density logs in negative velocity deviation zones. Negative deviation zones appear in dark blue to purple colors in Fig. 15.

Looking at the 2D porosity section the first thing draws attention is fairly low porosity distribution over the Asmari reservoir, but on the other hand when the reservoir production is reviewed, it is reported as a prolific reservoir (according to wells report, production rate of the studied zone is about 750 cubic meter per day). The only reason of such a high productivity is fractured development causing negative velocity deviations. In fact, fractures have a low role in the total porosity values, but even a small amount of fractures is really effective in reservoir permeability enhancement. Reservoirs with fracture usually produce more than expected.

5. Conclusion

In this study, through a series of sequential calculations on well log data, acoustic impedance and seismic attributes a section of velocity deviation was created over the Asmari Formation in the Hendijan oilfield. There is a good agreement between the results of petrographic studies and the well log derived pore types based on VDL. The Asmari Formation was divided into three zones based on seismic velocity deviation. Positive deviations greater than +500 m/s indicate isolated pore types such as moldic and vuggy porosities. Intercrystalline and microporosities are the main causers of zero deviations between -500 and +500 m/s in VDL. Negative deviations under -500 are created as a result of the dominance of connected porosities and possibly fractures. Generally, Asmari Formation in the studied field is characterized by a frequency of low porosities and its high productivity is related to occurring of natural fractures.

It is expected to use the methodology described in this study for pore typing in other carbonate reservoirs to reduce the uncertainty related to reservoir static and dynamic models.

References

Anselmetti, F.S., Eberli, G.P., 1999. The velocity-deviation log: A tool to predict pore type and permeability trends in carbonate drill holes from sonic and porosity or density logs. *AAPG Bulletin (American Association of Petroleum Geologists)*, 83(2-3), pp.450–466.

Dezfoolian, M.A., Riahi, M.A., Kadkhodaie, A., 2013. Conversion of 3D seismic attributes to reservoir hydraulic flow units using a neural network approach: An example from the Kangan and Dalan carbonate reservoirs, the world's largest non-associated gas reservoirs, near the Persian Gulf. Earth Sciences Research Journal (University of Colombia Press), 17, 75-78.

Doyen, P., 2007. Seismic reservoir characterization: an earth modelling perspective. *Constraints*, p.2007. Available at: http://www.aseg.org.au/Events/EETposter.pdf.

Gavotti, P.E., Lawton, D.C., Margrave, G.F., Isaac, J.H., 2012. Post-stack inversion of the Hussar low frequency seismic data. CREWES Research Report, 24, 1-22.

Golsanami, N., Kadkhodaie, A., Erfani, A., 2015. Synthesis of capillary pressure curves from post stack seismic data with the use of intelligent estimators: A case study from the Iranian part of the South Pars gas field, Persian Gulf Basin. Applied Geophysics, 112, 215-225.

Hampson-Russell user's guide, 2014. Emerge module documentation. Veritas Co.

Hampson, D.P., Schuelke, J.S. & Quirein, J.A., 2001. Use of multiattribute transforms to predict log properties from seismic data. *GEOPHYSICS*, 66(1), pp.220–236. Available at: http://dx.doi.org/10.1190/1.1444899.

IOOC, 2007. Iranian Offshore Oil Company (IOOC), Geologicaal report of Hendijan oilfield, unpublished report. 147 p.

Kadkhodaie, A., Rezaee, MR., Rahimpour-Bonab, H., Chehrazi, A., 2009. Petrophysical data prediction from seismic attributes using a committee fuzzy inference system. Computers & Geosciences, 35, 2314-2330

Kosari, E., Ghareh-Cheloo, S., Kadkhodaie, A., Bahroudi, A., 2015. Fracture characterization by fusion of geophysical and geomechanical data: a case study from the Asmari reservoir, the Central Zagros fold-thrust belt. Journal of Geophysics and Engineering, 12, 130-143.

Masters, T., 1995. Neural, novel and hybrid algorithms for time series prediction. John Wiley & Sons, Inc. New York, NY, USA

Nourafkan, A., Kadkhodaie, A., 2015. Shear wave velocity estimation from conventional well log data by using a hybrid ant colony-fuzzy inference system: a case study from Cheshmeh-Khosh oilfield. Journal of Petroleum Science and Engineering, 127, 459-468.

Nouri-Taleghani, M., Kadkhodaie, A., Karimi-Khaledi, M., 2015. Determining hydraulic flow units using a hybrid neural network and multi-resolution graph-based clustering method: case study from South Pars Gasfied, Iran. Journal of Petroleum Geology, 38(2), 177-191

Ouenes, A., 2000. Practical application of fuzzy logic and neural networks to fractured reservoir characterization. *Computers & Geosciences*, 26(8), pp.953–962. Available at: http://www.sciencedirect.com/science/article/pii/S0098300400000315.

Pramanik A.G., Srivastava A.K., Singh V., Katiyar R., 2002. Stratigraphic interpretation using post stack seismic inversion: Case histories from Indian Basins‖, SEG International Exposition and 72nd Annual Meeting, October 6-11 2002.

Rogers, S.J. et al., 1992. Determination of Lithology from Well Logs Using a Neural Network (1). *AAPG bulletin*, 76(5), 731–739.

Schlumberger, 2009. log interpretation charts. Schlumberger, Texas, USA, 293p.

Specht, D.F., 1990. Probabilistic neural networks. Neural networks, 3(1), 109–118.

Wang, J.-S., Song, J.-D. & Gao, J., 2015. Rough Set-Probabilistic Neural Networks Fault Diagnosis Method of Polymerization Kettle Equipment Based on Shuffled Frog Leaping Algorithm. *Information*, 6(1), pp.49–68. Available at: http://www.mdpi.com/2078-2489/6/1/49/.

Wayne, M.A., 2008. *Geology of Carbonate Reservoirs: The Identifi cation, Description, and Characterization of Hydrocarbon Reservoirs in Carbonate Rocks*, John Wiley & Sons, Inc., Hoboken, New Jersey. chapters 3,6,7

Yarmohammadi, S., Kadkhodaie, A., Rahimpour-Bonab, H., Shirzadi, A., 2014. Seismic reservoir characterization of a deep water sandstone reservoir using hydraulic and electrical flow units: A case study from the Shah Deniz gas field, the South Caspian Sea. Journal of Petroleum Science and Engineering, 118, 52-60.

Wyllie, M.R., Gregory, A.R., Gardner, G.H.F. 1956. Elastic wave velocities in heterogeneous and porous media: Geophysics, 21 (1), 41–70.
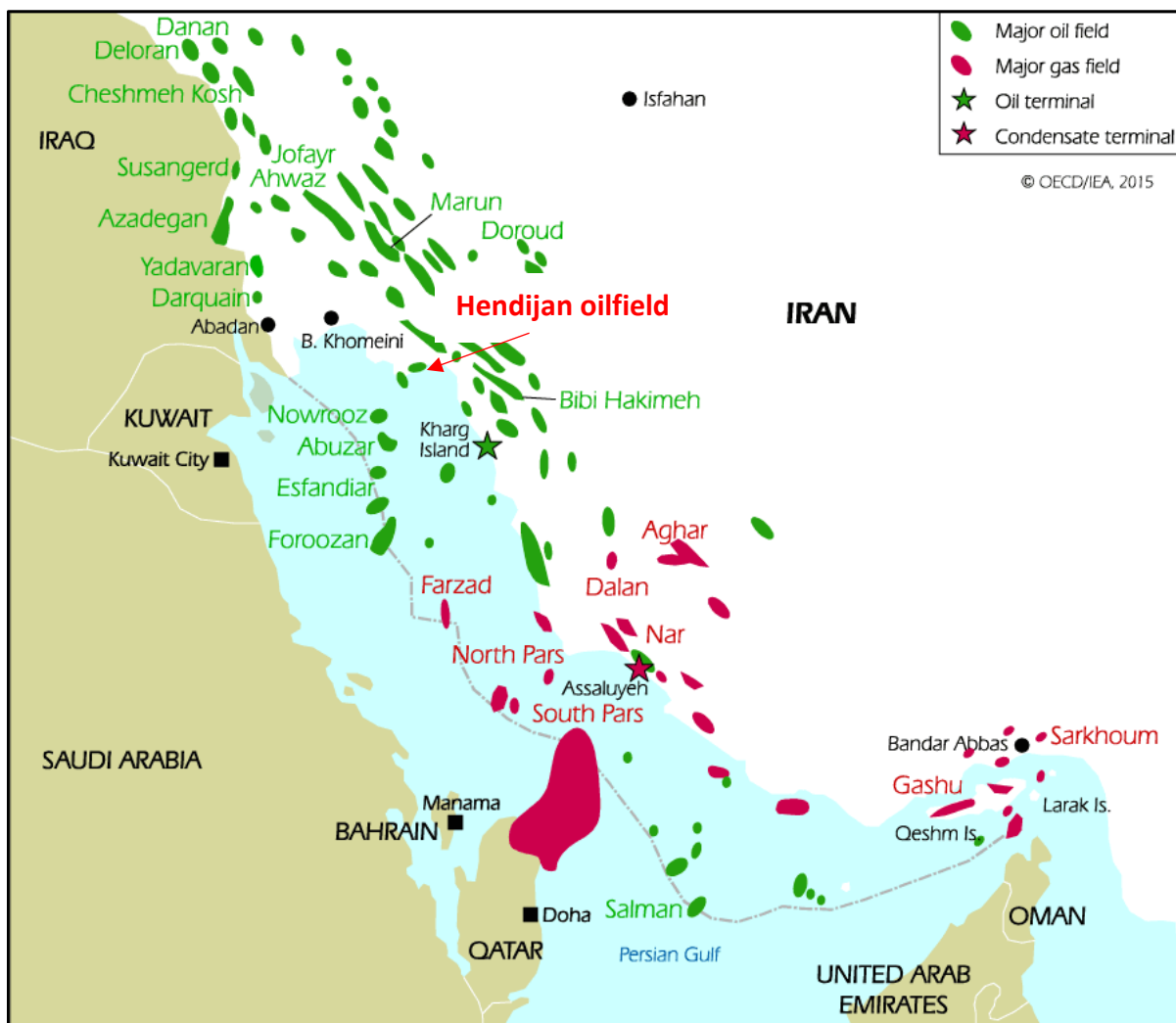
Fig. 1. Location map of the Hendijan oilfield in Persian Gulf (IOOC reports, 2007)
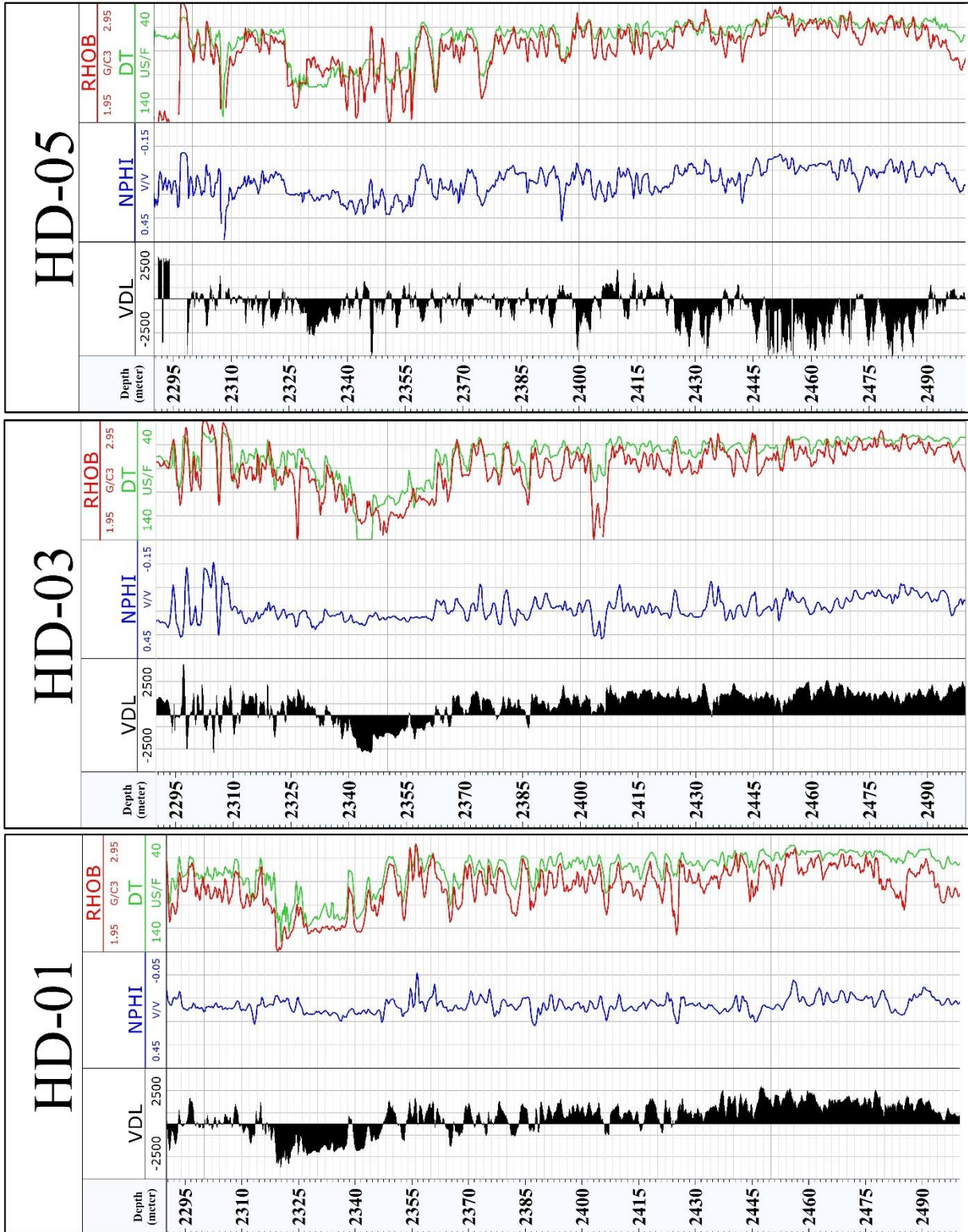
Fig. 1. Calculated VDL profiles (left track) in wells HD-01, HD-03 and HD-05 of Hendijan oilfield. Neutron log is displayed in middle track. Composite plot in right track represents overlay of sonic transit time and density logs.
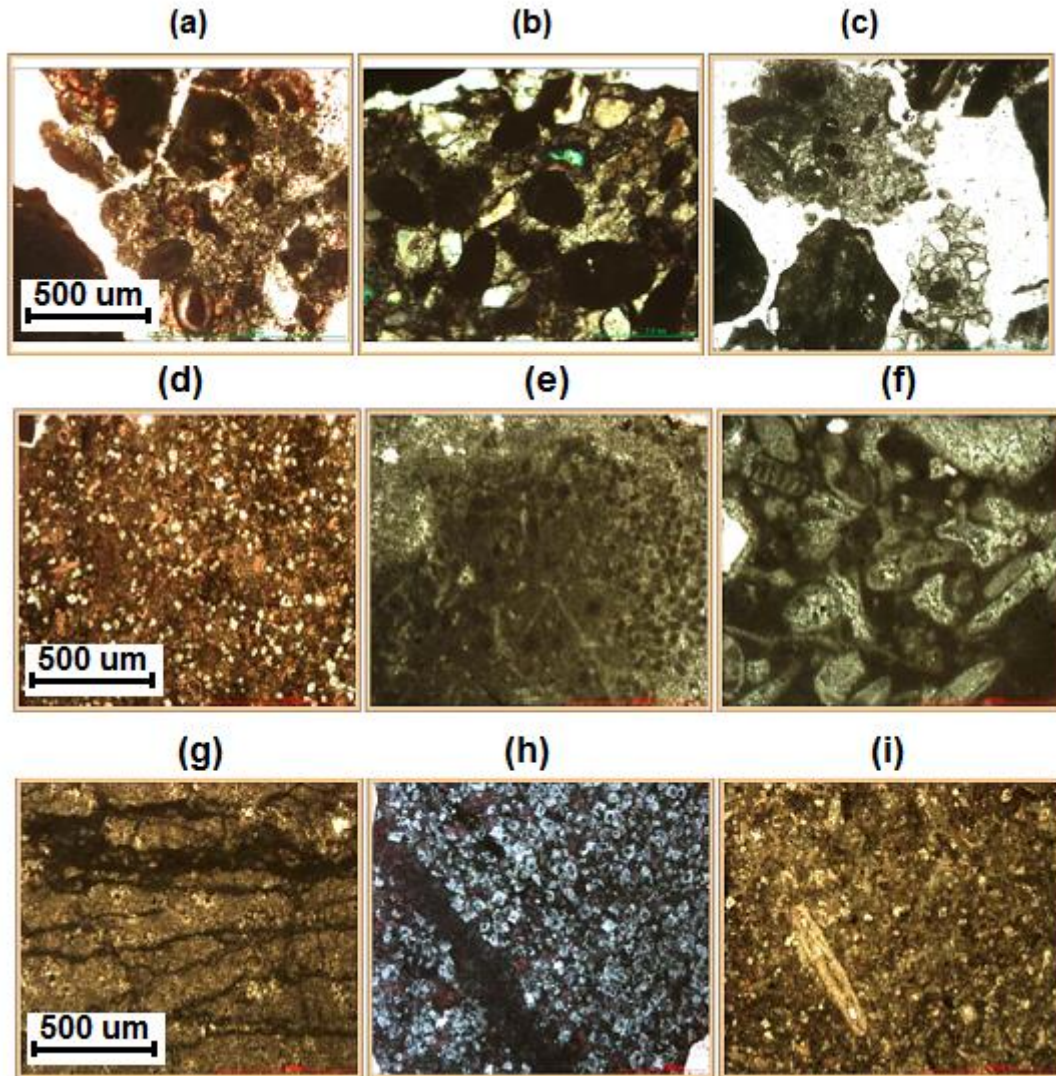
Fig.3. Photomicrographs showing different pore types of Asmari formation and their corresponding velocity deviation. Values inside the parenthesis indicate approximate velocity deviation for each microfacies. (a) bioclasic floatstone with microporosities (+250 m/s), (b) mixed carbonate/clastic microfacies with cemented porosities (+58 m/s), (c) bioclastic wackestone to packstone with some interpartcile porosities (-715 m/s), (d) dolomitized mudstone with intercrystalline and microporosities (-116 m/s), (e) peloidal packstone to wackestone with microporosity (-208 m/s), (f) bioclstic ooil grainstone with interparticle porosity (-1700 m/s), (g) fractured dolomudstone to wackestone (-2420 m/s), (h) dolomitic wackestone to packstone with clastic debris and intercrystalline porosity, (-492 m/s), (i) bioturbated mudstone to wackestone with microporosity (+435 m/s)
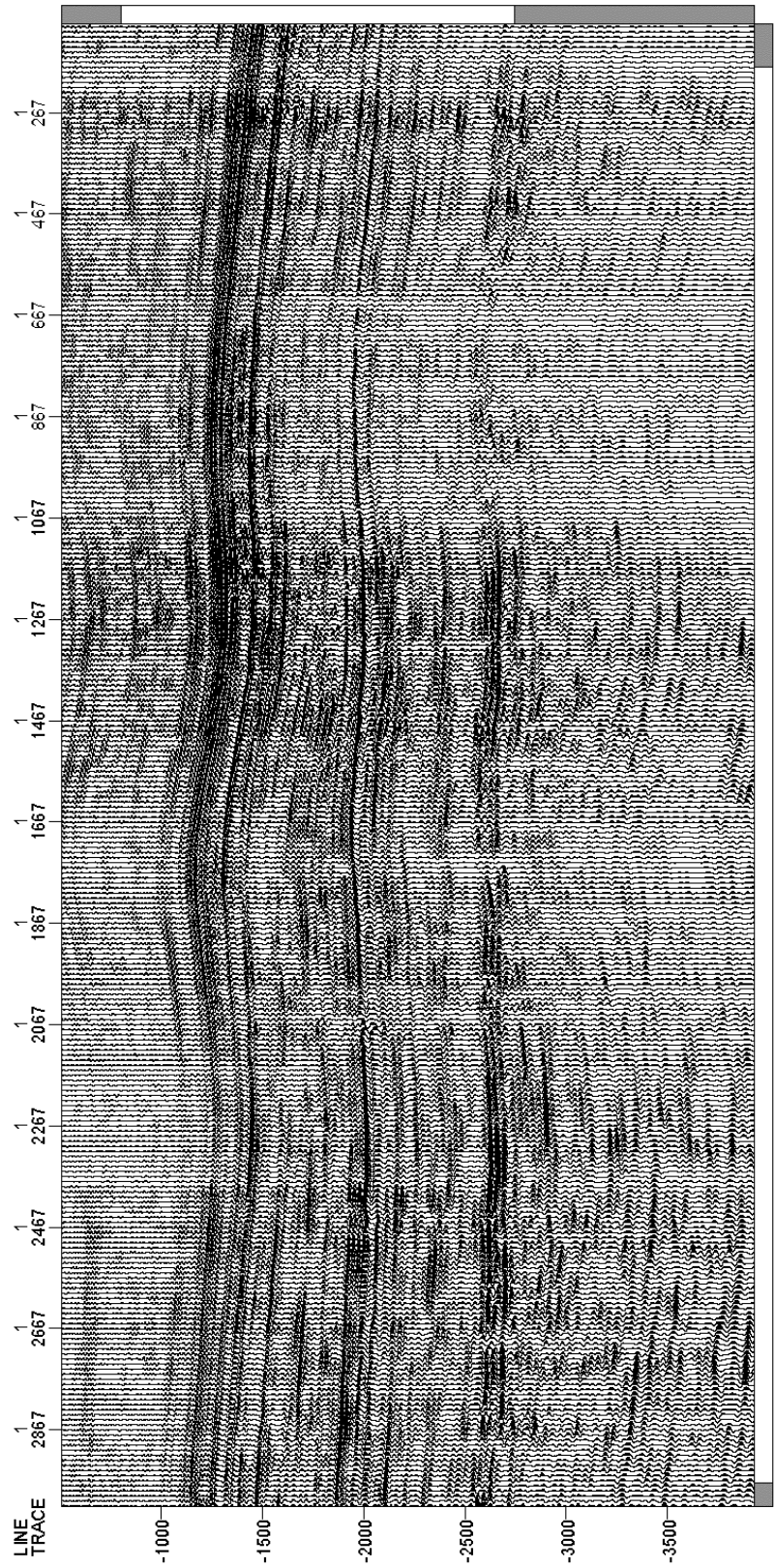
Fig. 4a. Seismic section showing general quality of post stack seismic data
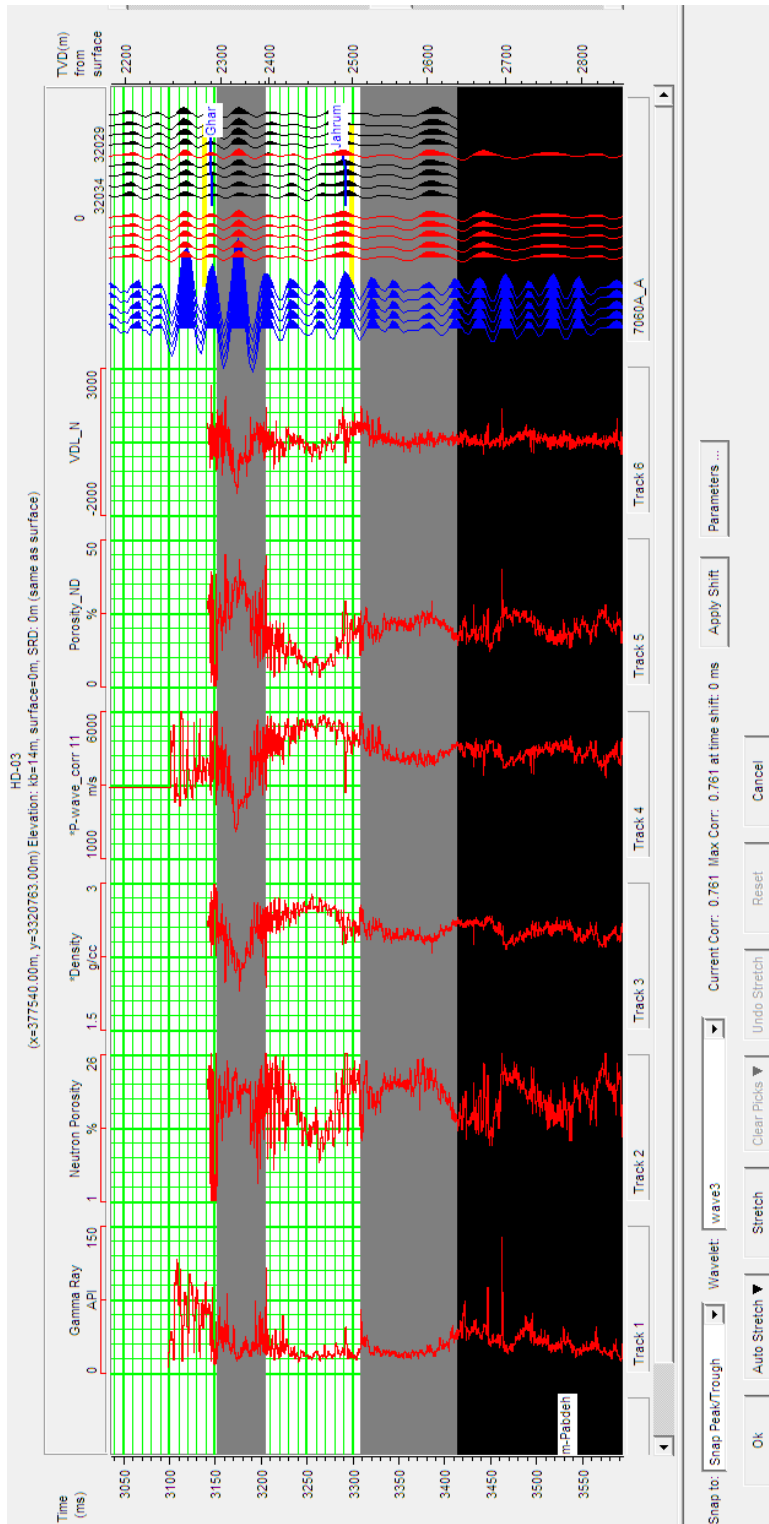
Fig. 4b. Synthetic seismogram showing well to seismic ties with correlation of 0.755, well HD-03. Gamma ray, neutron, density, sonic log, neutron-density and velocity deviations logs are show in track 1 through 6 from left. Right-side plots represent seismic section (black), composite trace (red) and synthetic seismogram (blue).
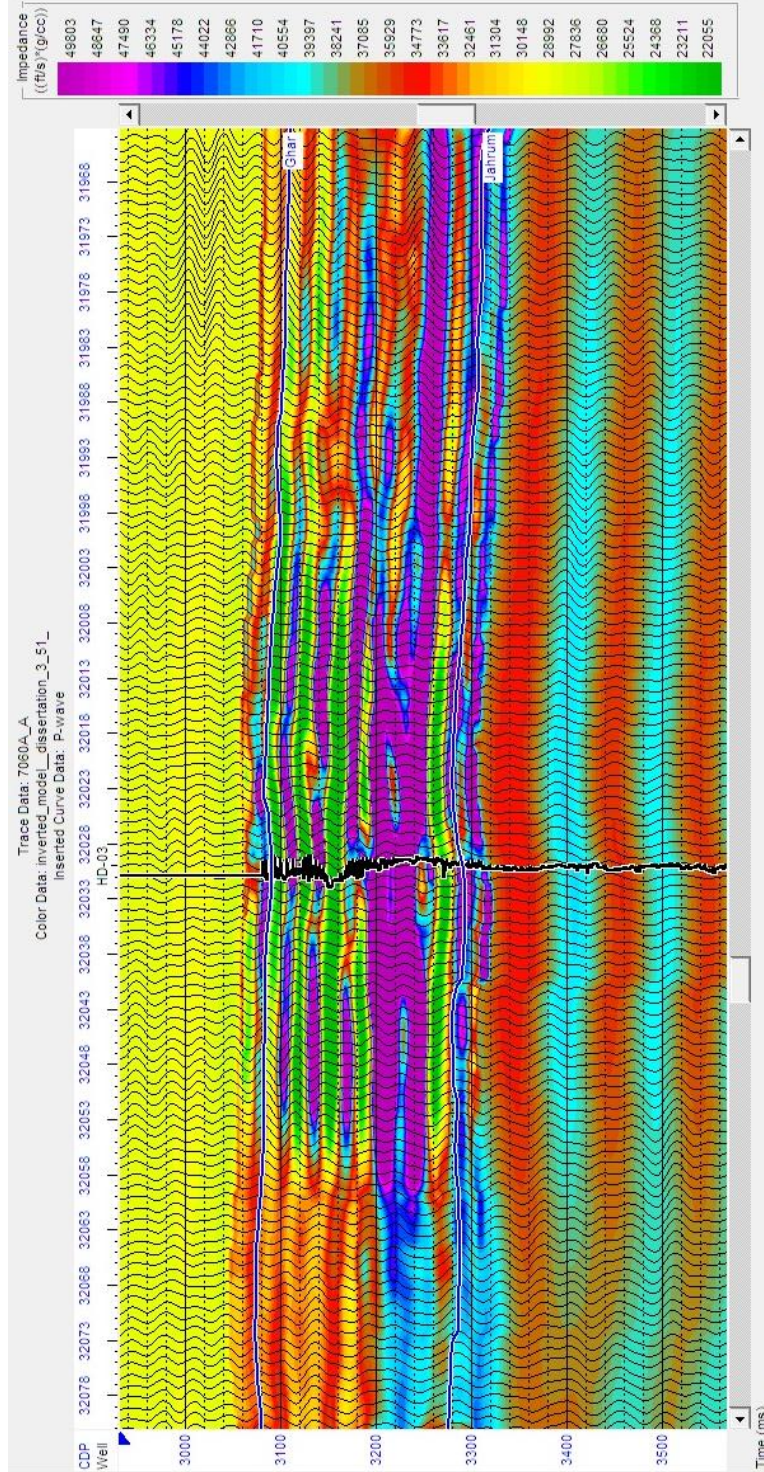
Fig. 5. A 2D section showing the results of acoustic impedance inversion. Ghar member of Asmari formation is generally characterized by low to medium acoustic impedance
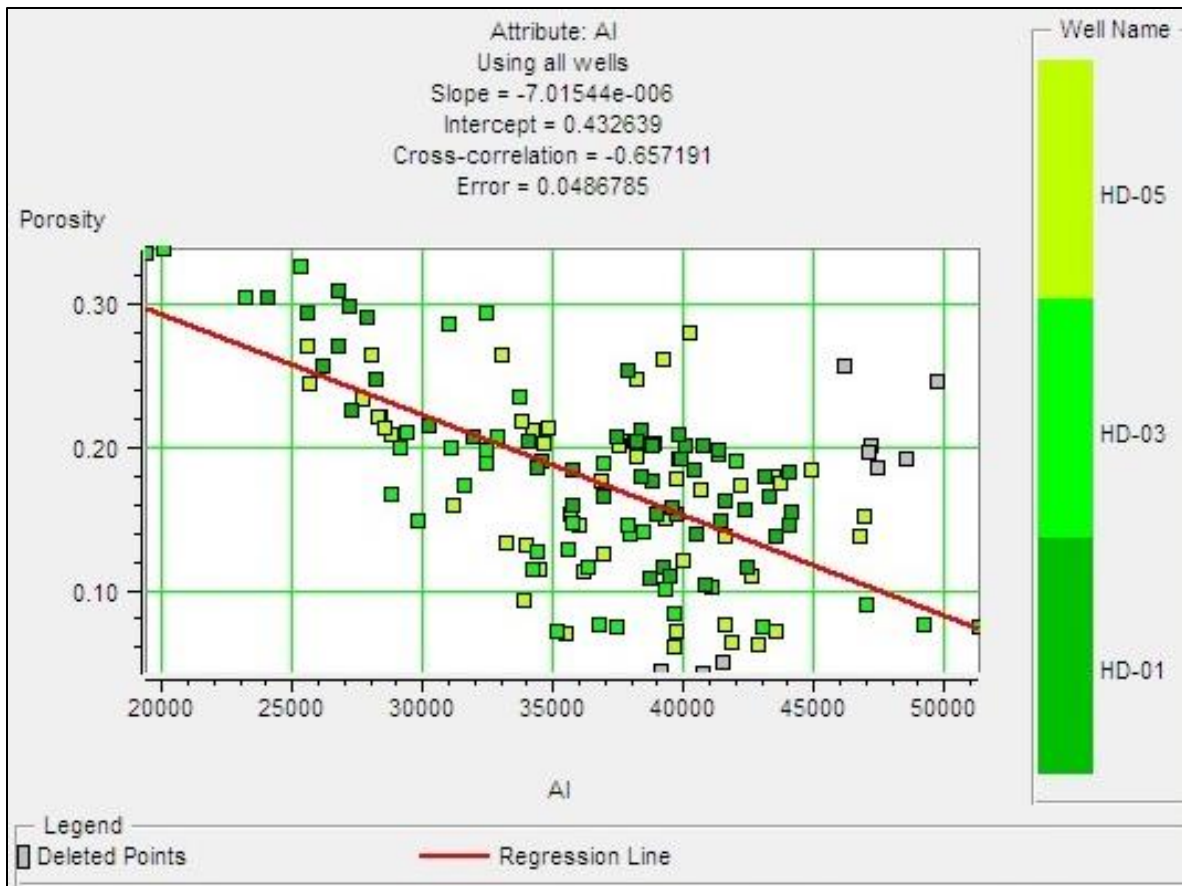
Fig. 6. Cross correlation between acoustic impedance calculated from seismic data and boreholes porosity. As is seen, acoustic impedance increases as porosity decreases. An inverse relationship with total correlation of -0.65 for three wells HD-01, HD-03 and HD-05 is achieved.
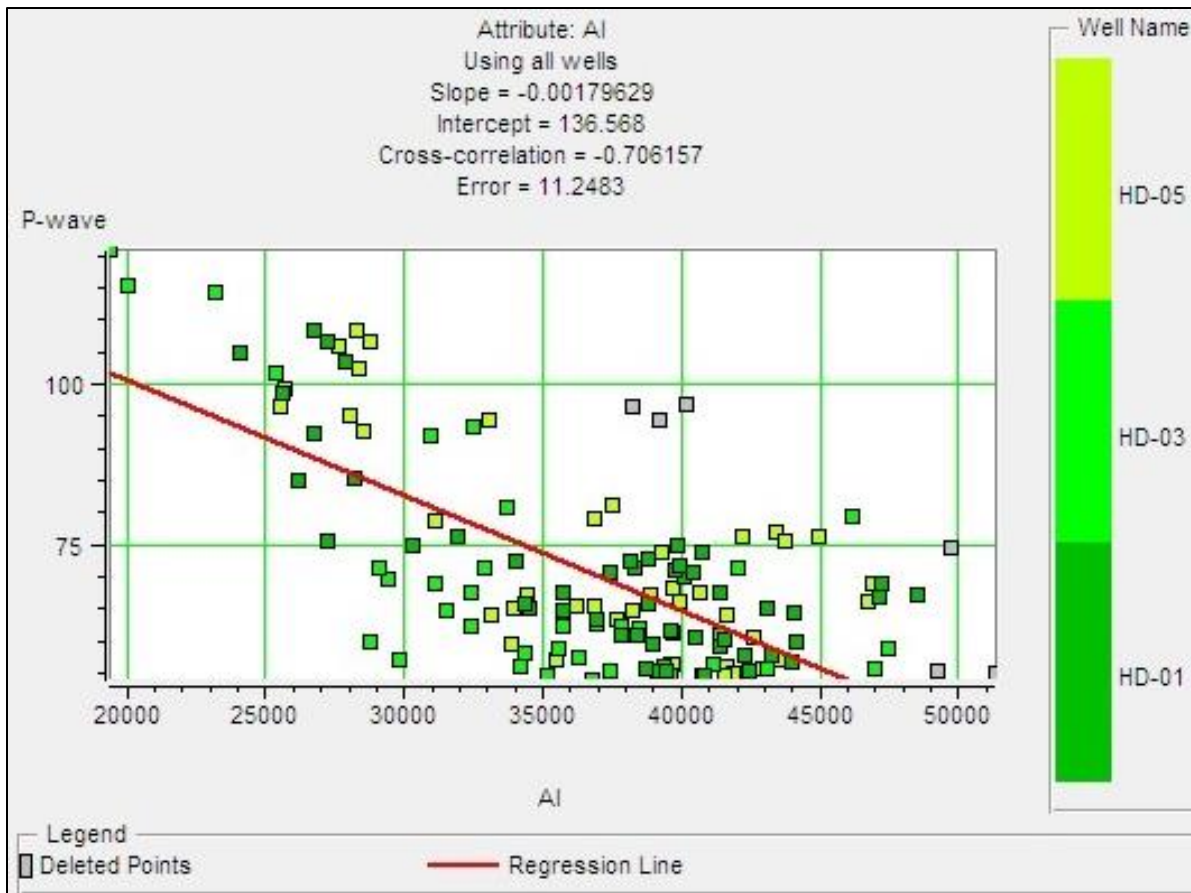
Fig. 7. Cross plot showing the correlation between acoustic impedance calculated from seismic data and sonic travel time at boreholes. As is seen, acoustic impedance increases as sonic transit time (P-wave) decreases. The relationship is inverse with a total correlation of -0.70 is three wells studied.
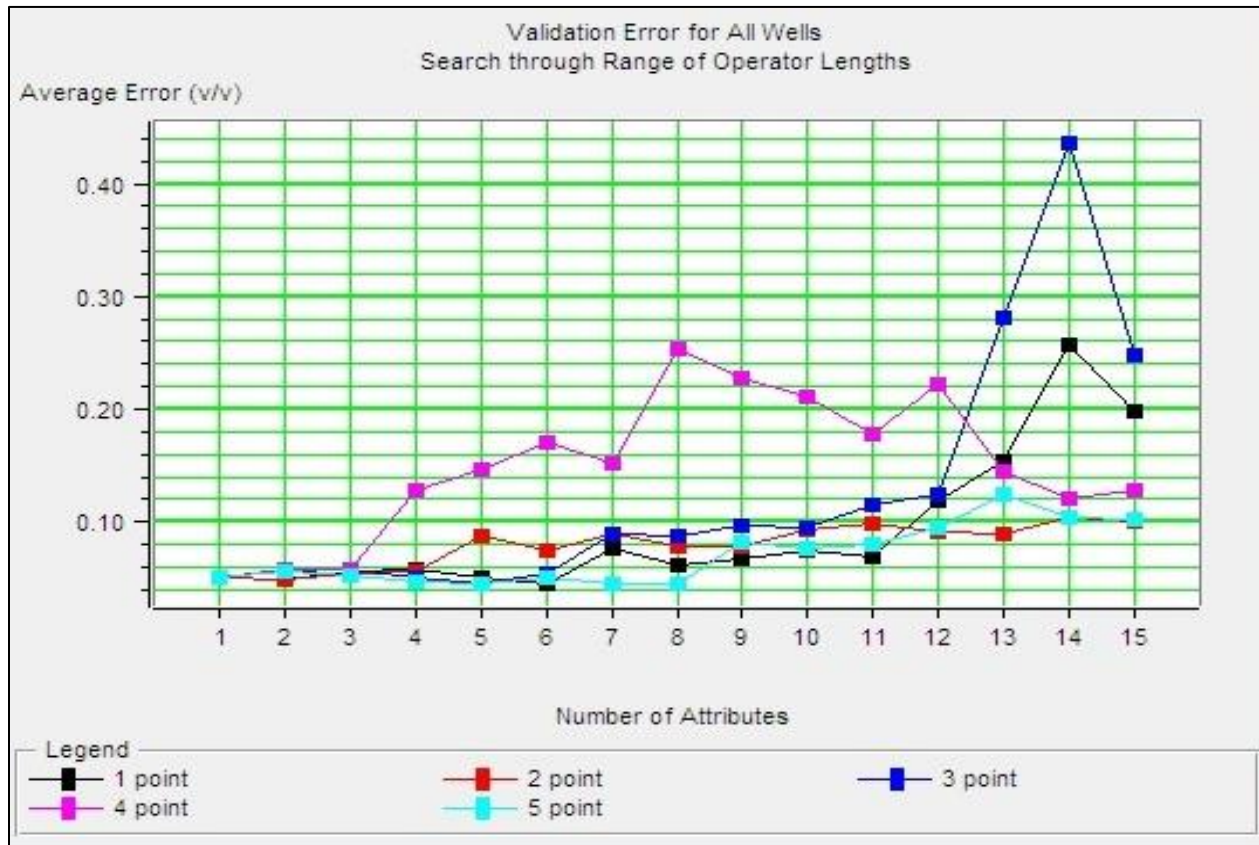
Fig. 8. Validation error for all wells versus number of attributes in porosity estimation model. Choosing a five point operator length is associated with least error and as shown after adding eight attributes validation errors starts to increase.
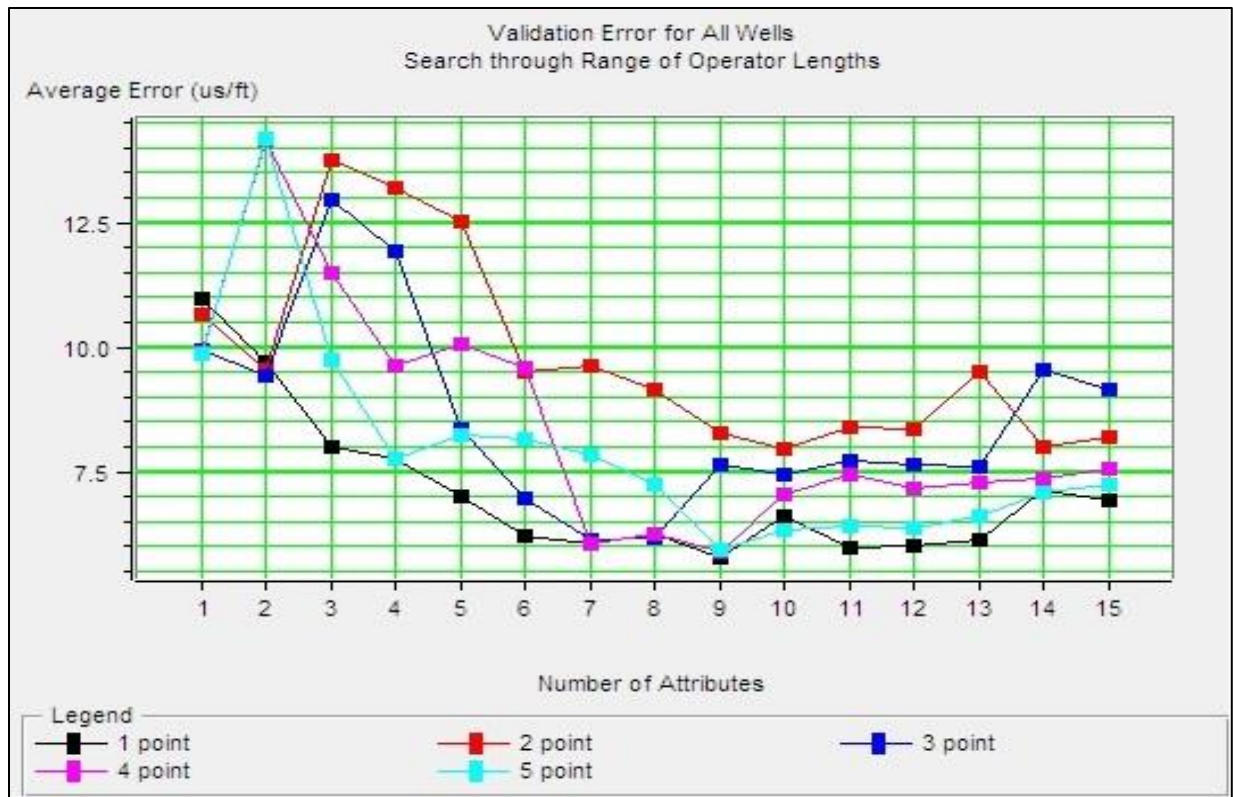
Fig. 9. Validation error for all wells versus number of attributes in sonic travel time estimation model. By using operator length =5, after adding nine attributes to input predictors list validation errors starts to increase.

Fig.10. Comparison between measured and estimated sonic transit time from seismic data at wells locations.
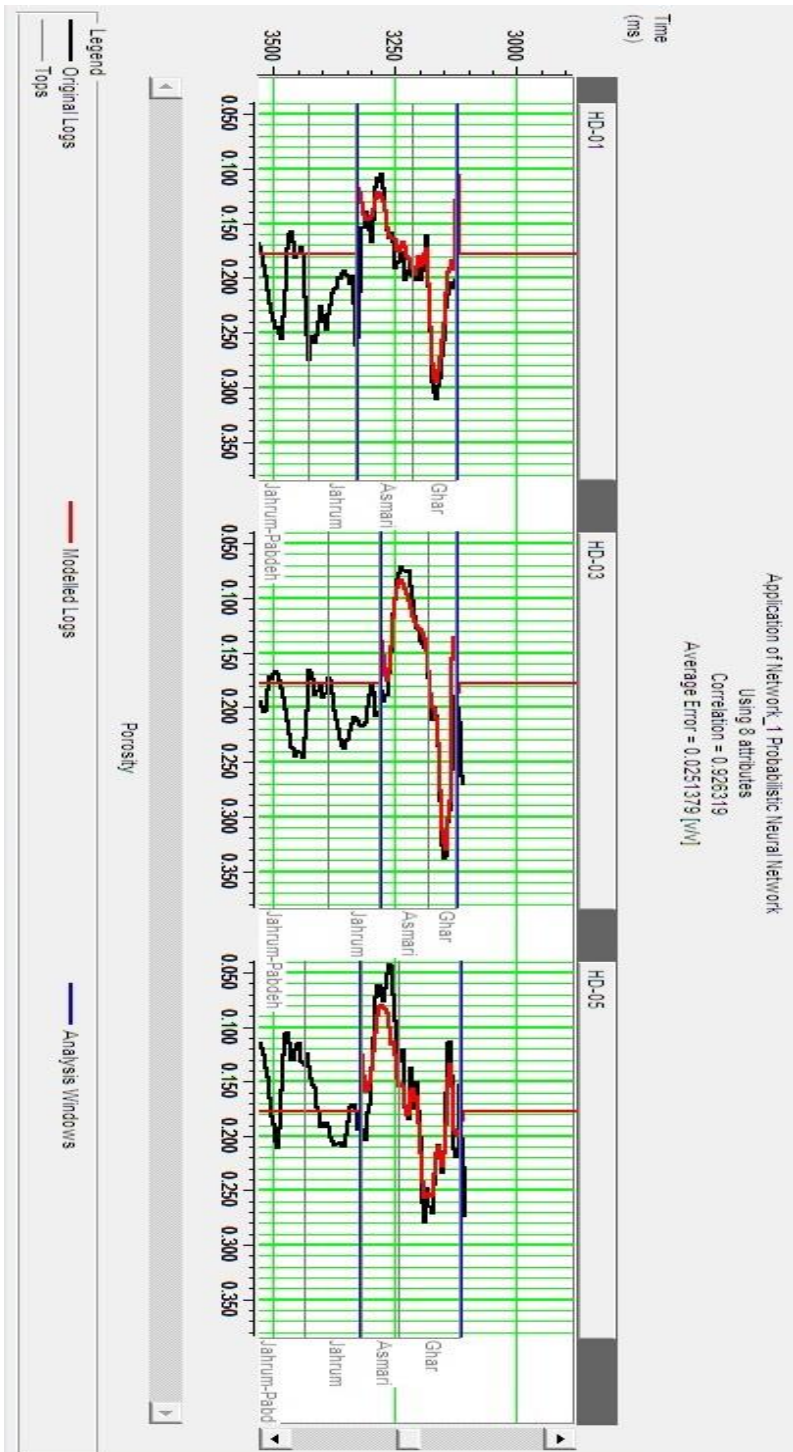
Fig.11. Comparison between measured and estimated sonic transit time from seismic data at wells locations.

create acoustic impedance section using suitable wavelet

extract best sets of attributes

making accurate neural network using sets of attributes

propagate sonic transit time and porosity from boreholes to seismic section

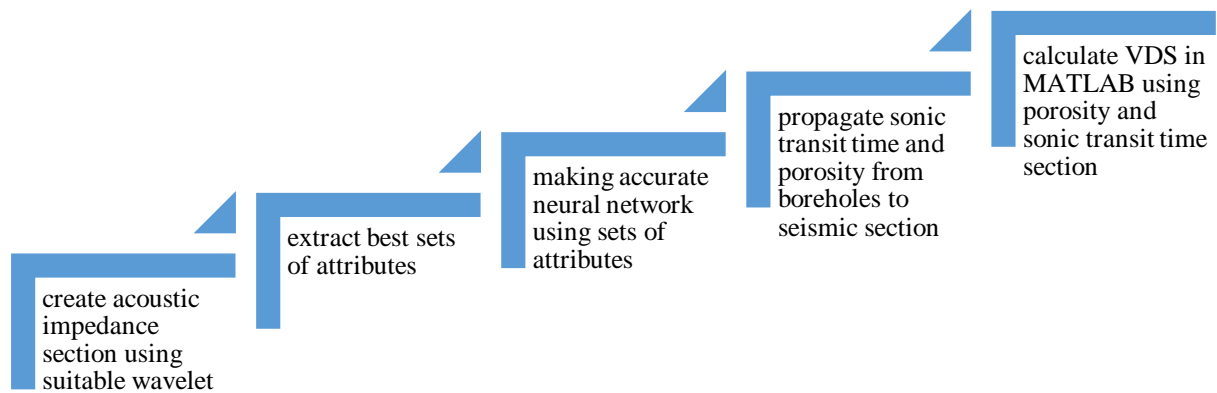calculate VDS in MATLAB using porosity and sonic transit time section

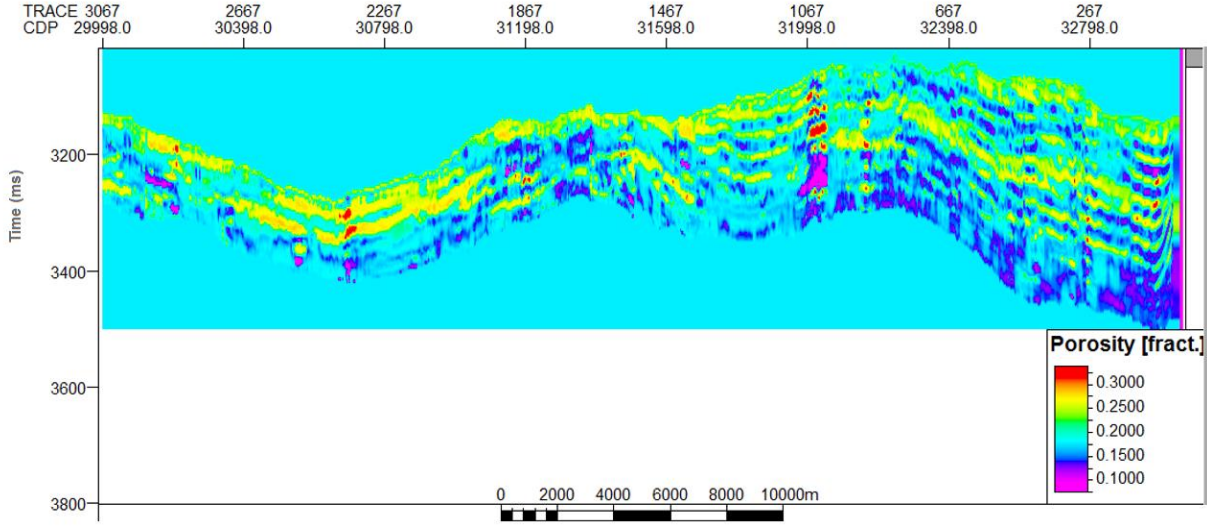**Fig.12.** Flow chart showing the computation steps to create VDS

Fig. 13. A 2D porosity section generated from eight seismic attributes by using PNN, Asmari reservoir. Generally, Asmari formation in the studied field is a low porosity reservoir and its high production rate is attributed to development of natural fractures. Changing colors from red to purple indicate reduction of porosities. In other words, the purple colored areas show the lowest porosities (0-0.12), and the red colored areas are associated with the high porosity zones (≥0.3), and the areas with light blue color are between them (0.2).
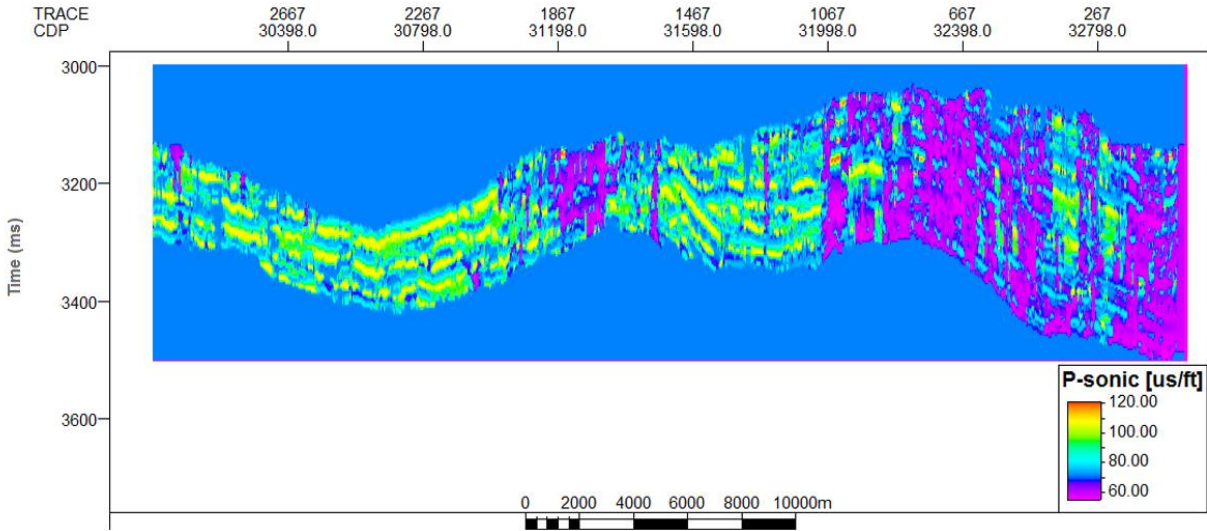
Fig. 14. 2D sonic travel time section generated from nine seismic attributes by using PNN, Asmari reservoir. As with the porosity, Asmari formation is generally characterized by low sonic transit time indicating lower porosities. Changing colors from red to purple indicates reduction of sonic travel time. Red color shows areas with the highest sonic transit time (~120 µs/f) indicating high porosities or fractured zones. Green and light blue color indicate areas with average sonic transit time related to fairly low porosity and poorly advanced fracture areas. Because of the lithology (carbonate formation) and low porosity in this formation as it is seen, most of the formation areas located in this part. Purple and dark blue areas, indicate very low porosities. Purple areas are indicative of carbonate rocks with nearly nil porosity (almost 50 µs/f).
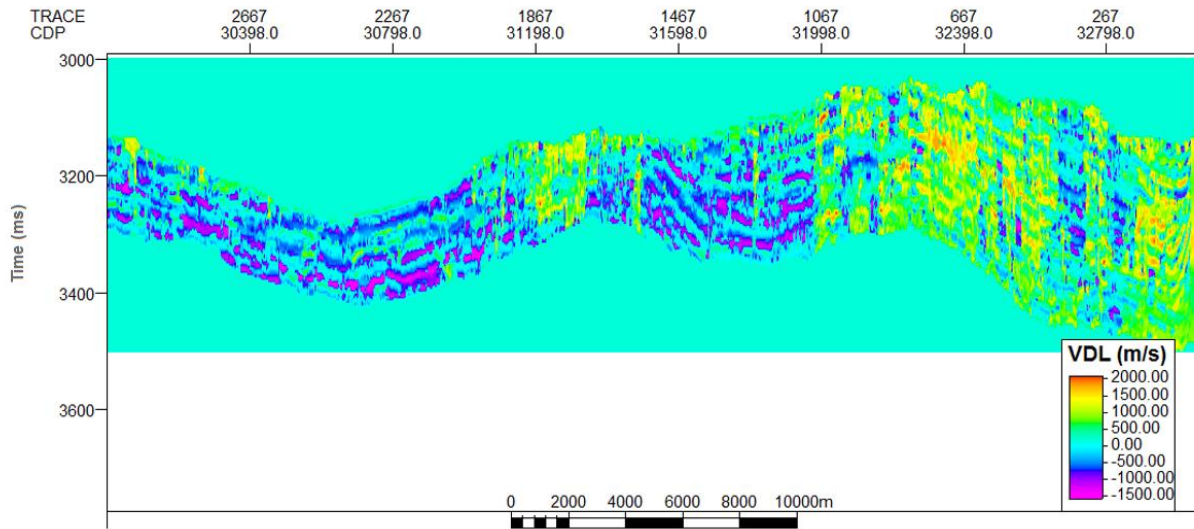
Fig. 15. Generated seismic velocity deviation section from total porosity and sonic transit time sections. Changing colors from red to purple shows reduction of velocity deviation from positive to negative amount. Red, yellow, and green coloured areas refer to isolated porosities without fractures (positive deviation). Blue and light blue zones refer to areas with almost nil velocity deviation indicating intergranular or microporosities. Connected and fractured zones are shown by dark blue and purple, the darker the color, the more fractured (negative deviations).

Appendix 1

Probabilistic neural network

Probabilistic neural network (PNN) is an alternative type of neural network (Masters, 1995; Specht, 1990). The probabilistic neural network (PNN) is actually a mathematical interpolation scheme which happens to use a neural network architecture for its implementation. The data used by PNN consist of a series of training examples, one for each seismic sample from all of the wells (Specht, 1990, Hampson-Russell user's guide, 2014):

$$
\begin{aligned}
&\{A_{11}, \quad A_{21}, \quad A_{31}, \quad L_1\} \\
&\{A_{12}, \quad A_{22}, \quad A_{32}, \quad L_2\} \\
&\{A_{13}, \quad A_{23}, \quad A_{33}, \quad L_3\} \\
&\qquad\vdots \\
&\{A_{1n}, \quad A_{2n}, \quad A_{3n}, \quad L_n\},
\end{aligned}
\tag{1}
$$

where there are n training examples and three attributes. The values L_i are the measured target log values for each of the examples. Given the training data, the PNN assumes that each new output log value can be written as a linear combination of the log values in the training data. For a new data sample with attribute values

$$
x = \{A_{1i}, \quad A_{2j}, \quad A_{3j}\},
\tag{2}
$$

the new log value is estimated as

$$
\hat{L}(x) = \frac{\sum_{i=1}^{n} L_i \exp(-D(x, x_i))}{\sum_{i=1}^{n} \exp(-D(x, x_i))},
\tag{3}
$$

Where

$$
D(x, x_i) = \sum_{i=1}^{3} \left(\frac{x_j - x_{ij}}{\sigma_j}\right)^2
\tag{4}
$$

The quantity $D(x, x_i)$ is the distance between the input point and each of the training points x_i. This distance is measured in the multi-dimensional space spanned by the attributes and is scaled by the quantity σ_j, which may differ for each of the attributes.

Equations (16) and (17) describe the application of the PNN network. The training of the network consists of determining the optimal set of smoothing parameters, σ_j. The criterion for determining these parameters is that the resulting network should have the lowest validation error.

Validation result for the m th target sample would be as

$$\hat{L}_m(x_m) = \frac{\sum\limits_{i \neq m} L_i \exp(-D(x_m, x_i))}{\sum\limits_{i \neq m}^{n} \exp(-D(x_m, x_i))} \tag{5}$$

This is the predicted value of the m th target sample when that sample is left out of the training data. Since we know the value of this sample, we can calculate the prediction error for that sample. Repeating this process for each of the training samples, we can define the total prediction error for the training data as

$$E_V(\sigma_1, \sigma_2, \sigma_3) = \sum\limits_{i=1}^{N} (L_i - \hat{L}_i)^2 \tag{6}$$

Note that the prediction error depends on the choice of the parameters σ_j. This quantity is minimized using a nonlinear conjugate gradient algorithm described in Masters, (1995). The resulting network has the property that the validation error is minimized.

Appendix 2

MATLAB codes used for calculating velocity deviation section

```matlab
clc;clear all;close all
%%
% construction of the seismic VDL section
% input parameters :
% Vp_real : seismic P_wave velocity
% phi : prosity
%% loading dta
dt_real = altreadsegy('cropped_DT_nn.segy');
phi = altreadsegy('cropped_porosity_nn.segy');
 %% calculations
dt_syn = 190*phi+49*(eye(size(phi))-phi);
Vp_syn = 304.8./dt_syn;


Vp_real = 304.8/dt_real; %km/s


vdl = 1000*(Vp_real-Vp_syn); % m/s
%% plotting results
[m,n] = size(vdl);
y = linspace(3000,3500,m);
x = linspace(0,3067,n);
imagesc(x,y,vdl);colorbar;colormap('ject')


% end of the main program

% The following codes read 2D seismic data in SEGY format. The codes for
reading 2D seismic section are actually adopted from CREWS project which is

written primarily by Gary F. Margrave (margrave@ucalgary.ca).

function [dataout, sampint, varargout] = altreadsegy(sgyfile, varargin)
 property_strings = ...

{'textformat','fpformat','segfmt','traces','times','depths','textheader','tra
ceheader','verbose','nt'};
 argout=0;
 verbose = FindValue('verbose',property_strings,varargin{:});
 if (~ischar(sgyfile))
    error('First argument must be a file name');
end
 fileinfo = dir(sgyfile); % Fileinfo is a structured array of file
information.
 if isempty(fileinfo)
    error(['The file ', sgyfile, ' does not exist.'])
end
 fileinfo.bytes; % Pull the size of the file out of fileinfo.
 gotDataFormat = 0;
byteOrder = 'be';    % Big-endian byte order
 while ~gotDataFormat
    fid = fopen(sgyfile, 'r', ['ieee-' byteOrder]);% Open the segy file for
reading.
     if fid == -1
        error('Unable to open file.')
    end
     % Read the segy file text header.  Even if the user doesn't want
     % the text header returned, we still load it and analyse it.
     % It will give us a clue about floating point format later on.
```

```matlab
    textheader = char(reshape(fread(fid, 3200, 'uchar'), 80, 40))';
    isEbcdic = FindValue('textformat', property_strings, varargin{:});
    if isempty(isEbcdic)
        % Convert from EBCDIC to ASCII if appropriate.
        % EBCDIC headers have byte values greater than 127 within them.
        isEbcdic = length(find(textheader > 127)) > 0;
        if verbose > 1
            disp('guessing the text header is ebcdic');
        end
    else
        switch isEbcdic
        case 'ebcdic'
            isEbcdic = 1;
        case 'ascii'
            isEbcdic = 0;
        otherwise
            error('Invalid text format specified.  Allowed values: ascii,
ebcdic');
        end
    end

    if isEbcdic
        textheader = ebcdic2ascii(textheader);
    end
     wantTextHeader =
BooleanValue(FindValue('textheader',property_strings,varargin{:}));
    if wantTextHeader
        argout = argout + 1;
        if nargout - 3 < 0
            error('Not enough output arguments to store text header');
        end
        textheaderarg = argout;
        varargout{1} = textheader;
    end
    % Read out the information from the binary header that is typically
available.
    % Header descriptions are in header.m.
    binpart1 = fread(fid, 3, 'int32'); % First section of the binary header.
    binpart2 = fread(fid, 24, 'int16'); % Second section of the binary
header.
     binaryheader = [ binpart1; binpart2];
     segfmt = binaryheader(10);
     fpformat = FindValue('fpformat', property_strings, varargin{:});
     switch segfmt
    case 1
      % If the text is ascii, there's a good chance the data is IEEE and not
IBM floating point
      % (If you're going to ignore the standard in one place, chances are
you'll ignore it in other places).
      if isempty(fpformat)
        if isEbcdic
            fpformat='ibm';
        else
            fpformat='ieee';
        end
      else
        if ~strcmp(fpformat,'ieee') & ~strcmp(fpformat,'ibm')
            error('Floating point format must be "ieee" or "ibm"');
        end
      end
      dformat = 'float32'; % 4 bytes, should be IBM floating point
      bytesPerSample=4;
      gotDataFormat=1;
    case 2
      dformat = 'int32'; % 4 bytes, signed.
      bytesPerSample=4;
      gotDataFormat=1;
    case 3
      dformat = 'int16'; % 2 bytes, signed.
      bytesPerSample=2;
      gotDataFormat=1;
    case 4
```

```matlab
          error('Can not read this format. (Fixed point with gain code.)');
      case 5
        if isempty(fpformat)
            fpformat='ieee';
        end
        dformat = 'float32'; % 4 bytes presumably IEEE floating point
        bytesPerSample=4;
        gotDataFormat=1;
      case 8
        dformat = 'uchar8'; % 4 bytes presumably IEEE floating point
        bytesPerSample=1;
        gotDataFormat=1;
      otherwise
        if strcmp(byteOrder,'be')
            firstTimeSegFmt = segfmt;
            byteOrder = 'le';
            % We'll loop due to gotDataFormat being false
        else
            % Tried big-endian and little-endian byte orders, and still the
format looks bogus.
            error(['Invalid data format contained within SEG-Y file.  Allowable
values: 1,2,3,4,5,8.  Got: ', num2str(firstTimeSegFmt), ' as big-endian, and
' num2str(segfmt), ' as little-endian']);
        end
      end
 end
 sampint = binaryheader(6) / 1e6; % Sample interval in seconds (was
microseconds)
 numsamps = FindValue('nt', property_strings, varargin{:});
if isempty(numsamps)
  numsamps = binaryheader(8); % Number of samples.
  if verbose
      disp(['number of samples per trace (from bytes 3221-3222) is '
num2str(numsamps)]);
  end
  if numsamps < 1
    %peek ahead in the first trace header to find numsamps
    [th ,st] = fread(fid, 120, 'uint16');
    if st ~= 120
        error('File is too short to be a valid SEG-Y file - it must have got
truncated');
    end
    fseek(fid, -240, 'cof');    % zip back to where we were before the
previous fread
    numsamps = th(floor(115/2) + 1);
    if verbose
        disp('Hmm.  That can not be right, lets look in bytes 115-116 of the
first trace.');
        disp(['Well, that got us ' num2str(numsamps) ' samples per trace']);
    end
  end
end
 if numsamps < 1
  error('Unable to determine the number of samples per trace - file is
corrupted or non-compliant with the SEG-Y standard. Try overriding with
<numsamps> parameter.');
end
 if verbose > 1
    disp(['using seg-y format number ' num2str(segfmt) ' - reading as '
dformat]);
    disp(['fpformat is ' fpformat]);
end
 % Check to see if the entire data set is to be read in or not.
traces = FindValue('traces',property_strings,varargin{:});
if isempty(traces)
    numtraces = floor((fileinfo.bytes-3600)/(240+(bytesPerSample*numsamps)));
    traces = 1:numtraces;
else
    numtraces = length(traces);
end
 numheaders=120;
dataout=zeros(numsamps,numtraces);
```

```matlab
traceheaders = zeros(numheaders,numtraces);
 for n=1:numtraces
    pos = 3600+((traces(n)-1)*(240+(bytesPerSample*numsamps)));
    st = fseek(fid, pos,-1);
    if st ~= 0
        break
    end
    [th ,st] = fread(fid, 120, 'uint16');
    if st ~= 120
        if verbose > 1
            disp(['File appears to be truncated after ' num2str(n) '
traces']);
        end
        break;
    end
    traceheaders(:, n) = th;

    if strcmp(fpformat,'ibm')
        [dataout(:,n) , st] = fread(fid, numsamps, 'uint32');
        if st ~= numsamps
            break;
        end
        dataout(:,n) = ibm2ieee(dataout(:,n));
    else
        [tmp, st] = fread(fid, numsamps, dformat);
        if st ~= numsamps
            break
        end
        dataout(:,n) = tmp;
    end
end
 fclose(fid);
  % -----------------------
function value = FindValue( property_name, property_strings, varargin )
 value = [];
for i = 1:((nargin-2)/2)
    current_name = varargin{2*i-1};
    if ischar(current_name)
        imatch = strmatch(lower(current_name),property_strings);
        nmatch = length(imatch);
        if nmatch > 1
                error(['Ambiguous property name ' current_name '.']);
        end
        if nmatch == 1
            canonical_name = property_strings{imatch};
            if strcmp(canonical_name, property_name)
                if isempty(value)
                    if isempty(varargin{2*i})
                        error(['Empty value for ' property_name '.']);
                    end
                    value = varargin{2*i};
                else
                    error(['Property ' property_name ' is specified more than
once.']);
                end
            end
        end
    end
end
%---------------------
 function value = BooleanValue(x)

if ischar(x)
    x = lower(x);
    value = strcmp(x,'yes') | strcmp(x, 'on') | strcmp(x, 'true');
elseif ~isempty(x) & isnumeric(x)
    value = (x ~= 0);
else
    value = 0;
end
```